Showcasing research from Dr. Ashok Keerthi's laboratory, Department of Chemistry, The University of Manchester, United Kingdom.

Microtomy-fabricated two-dimensional nano-slits enable single molecule biosensing

An ultramicrotomy-based slicing method has been developed to produce several hundreds of identical 2D nano-slit devices with atomic-scale precision—a major advancement in nanofabrication that overcomes longstanding challenges in throughput and reproducibility. This precise and scalable technique enables the fabrication of MoS_2-based 2D nano-slits capable of real-time detection of individual DNA molecules, capturing intricate molecular conformations *via* the resistive pulse sensing technique. The approach offers a powerful platform for high-throughput biomolecule sensing and unlocks new opportunities for advanced diagnostics and nanofluidic technologies.

Image reproduced by permission of Muhammad Sajeer P, Ankit Bhardwaj, Boya Radha, Manoj Varma and Ashok Keerthi from *Nanoscale*, 2025, **17**, 18605.

Image created using Microsoft Copilot and Blender (www.blender.org).

As featured in:

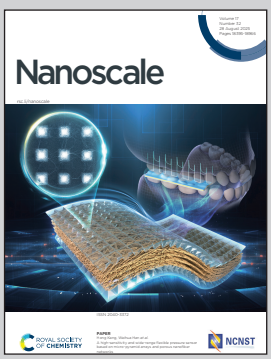

See Boya Radha, Manoj Varma, Ashok Keerthi *et al.*, *Nanoscale*, 2025, **17**, 18605.

ROYAL SOCIETY OF CHEMISTRY

rsc.li/nanoscale

Registered charity number: 207890

Nanoscale

PAPER

View Article Online
View Journal | View Issue

Cite this: *Nanoscale*, 2025, **17**, 18605

Microtomy-fabricated two-dimensional nano-slits enable single molecule biosensing†

Muhammad Sajeer P, [a,b,c,d] Ankit Bhardwaj, [b,d] Boya Radha, [*b,d,e] Manoj Varma [*c] and Ashok Keerthi [*a,d,e]

Nanofluidic devices have emerged as a powerful sensor for single-molecule studies. Among these, biological nanopores have demonstrated remarkable capabilities, ranging from detecting epigenetic modifications in DNA to showing promising results for developing protein sequencing technologies. Despite extensive research, their solid-state counterparts, such as solid-state nanopores and nano-slits, have not achieved comparable success. Unlike biological nanopores, where bacterial proteins can spontaneously insert into lipid membranes to create thousands of atomically identical copies, their solid-state counterparts lack a similarly straightforward and scalable fabrication method. This inability to consistently produce multiple devices with the same precision in dimensions as biological systems remains a significant barrier to their academic and industrial adoption and applications in molecular sensing. Towards this direction, we show the potential of ultramicrotomy-based fabrication of atomically smooth two-dimensional (2D) nanocapillaries and their applications in biosensing. This precise and straightforward method enabled the sustainable production of several hundred molybdenum disulfide-based 2D nano-slits with identical cross-sectional dimensions and tunable lengths from layered crystals. Here, we demonstrated DNA sensing with these 2D nano-slits using the resistive ionic current blockade technique. This robust microtomy technique accelerates production from a single device over 2–3 weeks to hundreds of identical nano-slit biosensors in parallel within the same period. In addition to $1/f$ noise analysis, these MoS_2 nano-slits reveal diverse topological local conformations of DNA during translocation.

Received 4th May 2025,
Accepted 10th July 2025

DOI: 10.1039/d5nr01832c

rsc.li/nanoscale

Introduction

Developing tools for ultrasensitive single-molecule studies is crucial, particularly in biology. The nano-fluidic devices, such as nanopores and nano-slits, have emerged as a promising toolbox for studying on a single molecule level.[1] These devices have shown potential applications such as DNA sensing[2–5] and sequencing[6] to proof of concepts in developing protein sequencing techniques.[7–9] For instance, biological nanopores have already been successfully commercialized for DNA sequencing and established as a major part of the next generation sequencing tools. In contrast, even though solid-state nanopores offer chemical, mechanical and thermal stability over biological nanopores, they are yet to prove their practical viability for DNA sequencing. A few among the major challenges include the difficulty in reproducing solid-state nanopores with atomic precision in dimensions and a lack of control over the translocation speed of biopolymers through the pore. On the other hand, synthetic nano-slits are also gaining momentum for their applications in bio-sensing and studies on structural configurations as well as translocation dynamics of biopolymers.[2,3] Given these increasing academic and industrial interests[10] and to aid further exploratory research, various fabrication techniques have been developed since the late 20th century.

Traditionally, solid-state nanopores are drilled solely on free-standing membranes of silicon, silicon nitride or other 2D materials using a mix of techniques such as transmission electron microscopy (TEM), focused ion beam (FIB), or dielectric breakdown.[11–14] Nano-slits, on the other hand, are produced through either top-down or bottom-up approaches.[15] These include molecular self-assembly, lithography, and chemical routes.[16] In the context of bio-sensing applications on an industrial level, particularly for DNA sensing, the ability to

[a]*Department of Chemistry, School of Natural Sciences, The University of Manchester, Manchester M13 9PL, UK. E-mail: ashok.keerthi@manchester.ac.uk*
[b]*Department of Physics and Astronomy, School of Natural Sciences, The University of Manchester, Manchester, M13 9PL, UK. E-mail: radha.boya@manchester.ac.uk*
[c]*Center for Nanoscience and Engineering, Indian Institute of Science, 560012, India. E-mail: mvarma@iisc.ac.in*
[d]*National Graphene Institute, The University of Manchester, Manchester, M139PL, UK*
[e]*Photon Science Institute, The University of Manchester, Manchester M13 9PL, UK*
† Electronic supplementary information (ESI) available. See DOI: https://doi.org/10.1039/d5nr01832c

create nano-slits and nanopores with both precise control over their inner dimensions and scalability is important. Developing efficient and scalable fabrication methods that deliver nanopores/nano-slits with atomically smooth inner walls or constrictions is essential for further advancements in this field and industry adoption.[17]

In this study, we demonstrate the biosensing capabilities of 2D nano-slits, fabricated through a sustainable and scalable method.[18] This approach utilizes ultramicrotomy to slice 2D capillaries, which are constructed from molybdenum disulfide (MoS_2) 2D crystals. This precise method allowed us to detect DNA translocation through MoS_2-based 2D nano-slits using the resistive ionic current blockade technique. MoS_2 is particularly interesting compared to other 2D materials due to several reasons, such as better optoelectronic properties.[19] It also has better chemical tunability compared to graphene,[20] owing to its reactive sulfur atoms enabling different surface chemistries, making it useful for selective sensing of biomolecules.[21,22] The low adhesion of DNA molecules to MoS_2 significantly mitigates channel clogging, enhancing the reliability of translocation measurements.[23,24] Several studies also depicted MoS_2 as a potential candidate for proteomics and genomics.[9,25–27]Hence, MoS_2 exhibits higher sensitivity in biomolecular sensing applications.[23,28,29] Apart from these reasons, MoS_2 is practically viable for use with the ultramicrotomy slicing technique, where graphite and hBN fail due to their weak interlayer forces and lubricity between layers as well as their poor cohesion with epoxy resin.[18]

In contrast to other techniques, ultramicrotomy-based production of 2D nano-slits works under atmospheric conditions and has the potential for scalable fabrication. For instance, conventional fabrication methods typically require 2–4 weeks to produce a single two-dimensional nano-slit device[15] based on the expertise. In contrast, once we prepare one of the layered crystal stacks on the epoxy resin block, we can fabricate hundreds of nanocapillary devices with minimal variability using the ultramicrotomy fabrication technique, significantly reducing both time and cost. For example, we were able to produce up to 200 nano-slits within 20 minutes.

While our prior study[18] introduced the ultramicrotomy technique for fabricating 2D channels, in this work, we implement this scalable fabrication approach for the first time for label-free detection of DNA. Prior work primarily focused on the fabrication of ultrathin membranes, whereas this study explores their direct application in biosensing, filling an important gap. This transition from fabrication to functional application is a crucial step forward, establishing ultramicrotomy-assisted nano-slits as a powerful and scalable platform for nanofluidic biosensing. We have explored possible substrates with micropores such as silicon and silicon nitride (SiN_x) to fabricate 2D nano-slit devices for ion and bio-molecule transport (see the detailed description in the fabrication section) and re-cycling of substrates for sustainable fabrication, making this technique accessible for the wider scientific community. This method also offers utmost flexibility in defining the channel length and provides scope for the fabrication of multi-slit systems, which has attracted significant interest in DNA sensing recently.[30,31] By demonstrating DNA sensing using MoS_2-based 2D nano-slit devices fabricated *via* the ultramicrotomy technique, we aim to significantly advance the emerging biosensing applications that utilize synthetic nanochannels.[10]

Device fabrication

We employ ultramicrotomy to fabricate multiple 2D nano-slit devices with channel lengths of 300 nm from a single 2D nanocapillary, van der Waals (vdW) assembly containing a tri-crystal stack, using our reported procedure.[18] Our methodology commences with a vdW heterostructure incorporating top and bottom MoS_2 crystals with thickness ranging from 100 to 200 nm, wherein the middle MoS_2 crystal (thickness, 8.4 nm) has been lithographically patterned and etched to form parallel channels, defining its width (W = 100 nm) and height (H = 8.4 nm) with 250 nm spacing between them (Fig. 1E).[15] The middle/spacer crystal is sandwiched between the top and bottom MoS_2 crystals, with a few tens of microns in lateral dimensions, to result in 2D capillaries within the vdW assembly. This 2D capillary stack of MoS_2 crystals was fabricated in a cleanroom environment and then embedded in the epoxy resin under ambient conditions. The epoxy resin block containing 2D nanocapillaries was subsequently sectioned using ultramicrotomy (Fig. 1A), yielding numerous membrane slices (300 nm thickness, which is the channel length L for 2D nano-slits). The sliced resins were collected using a poly(propylene) carbonate film coated on a polydimethylsiloxane (PPC/PDMS) substrate (Fig. 1B) and then transferred to a 5×25 μm^2 micro-hole made on a 500 nm thick SiN_x membrane, which was fabricated using standard photolithography and dry etching techniques (Fig. 1C; also refer to ESI's† Methods section). Fig. 1F shows the optical microscopy image of the final device.

Ashok Keerthi

Dr Ashok Keerthi is a Presidential Academic Fellow in the Department of Chemistry at the University of Manchester. He obtained his PhD from the National University of Singapore in 2014, followed by postdoctoral research at the Max Planck Institute for Polymer Research (Germany) and the University of Manchester. In 2019, he was awarded the prestigious Ramsay Memorial Fellowship, followed by the Presidential Fellowship in 2022, enabling him to establish his independent research group. His current research focuses on the bottom-up synthesis of chiral nanographenes, graphene nanoribbons, and angstrom-scale channels. His group investigates the chemistry and physics of molecular architectures and 2D capillaries.

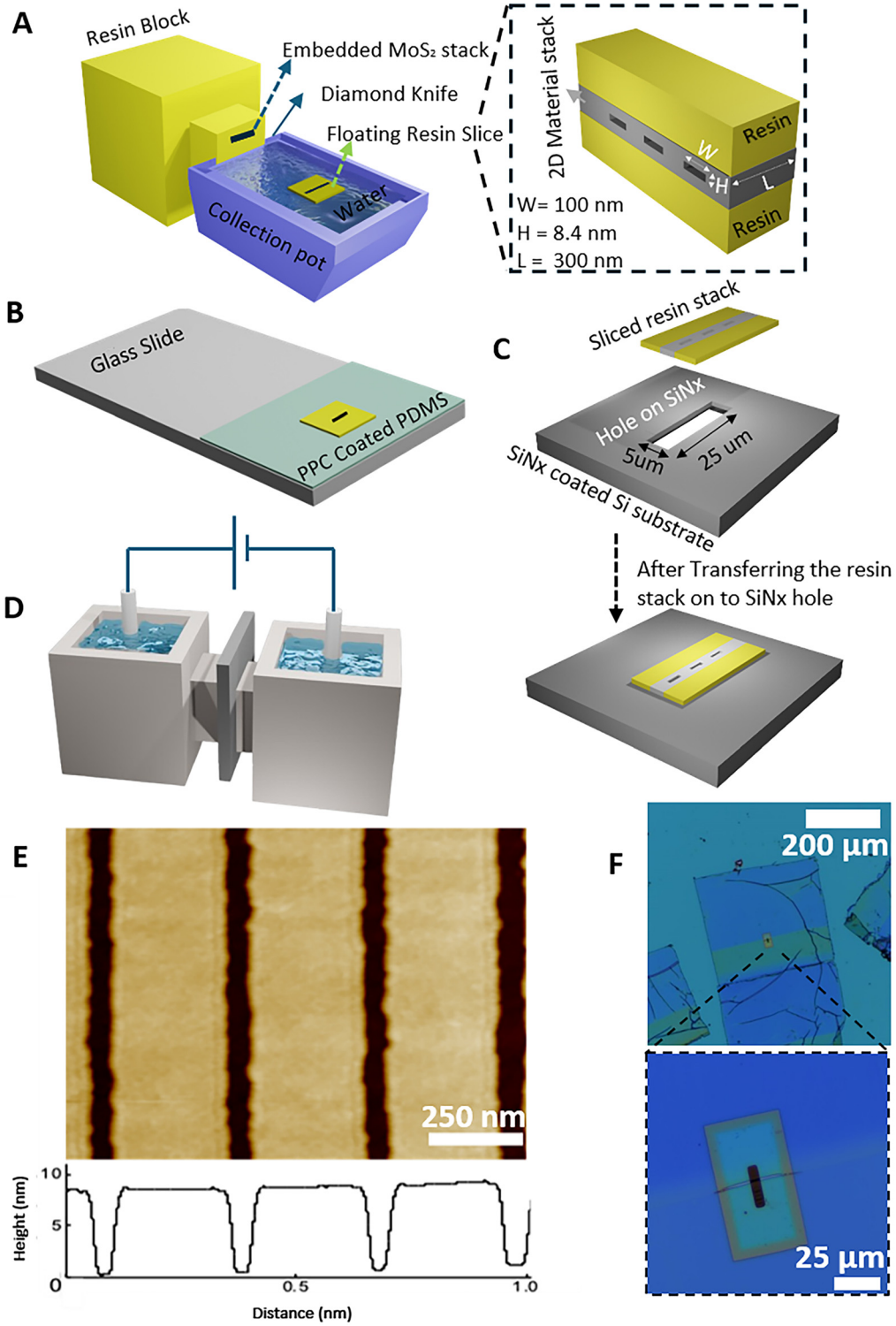

Fig. 1 Schematic illustration of 2D nano-slit device fabrication and the measurement setup. (A) Ultramicrotomy slicing of the MoS_2 vdW structure embedded inside a resin block using a diamond knife. An enlarged schematic of a sliced resin with dimensions of a 2D nano-slit. (B) The sliced resin is picked up using a PPC/PDMS substrate. (C) The sliced resin is transferred onto a SiN_x membrane with a pre-drilled hole. (D) Schematic of the voltage-biased custom-built PEEK flow cell used for ion and DNA translocation/sensing experiments with Ag/AgCl electrodes. (E) AFM image and the line scan profile of the etched channels on the MoS_2 spacer crystal. (F) Optical microscopy images of the MoS_2-based 2D nano-slit device.

DNA sensing with microtomy-fabricated MoS_2-based 2D nano-slits

The microtomy-fabricated 2D nano-slit device is sandwiched between custom-built polyether ether ketone (PEEK) flow cells, which are filled with 3 mL of 4 M LiCl aqueous electrolyte in both reservoirs (Fig. 1D). The LiCl electrolyte is used for improving the signal to noise ratio of the ionic current signal.[32] The standard Ag/AgCl electrodes are used for applying the voltage bias and to measure ionic current simultaneously, using an Axopatch 200B amplifier, which is controlled by a customized LABVIEW software program. To showcase the device's potential for DNA sensing applications, a 5000 base-pair DNA (no limit DNA fragments, product number: SM1731, Thermo Fisher Scientific) is used in a 4 M LiCl electrolyte with 40 mM Tris-HCl (AccuGene) and 4 mM EDTA (Flurochem) buffer solutions. For the experiment, 5 μL of stock solution (0.5 μg μL^{-1}) of DNA is injected into a negatively biased reservoir of the PEEK flow cell. The sampling is done at 100 kHz and later digitally filtered using a Gaussian low pass filter at 3 kHz. The data analysis is carried out with the standard Transalyzer MATLAB software package.[33]

Right after fabrication, the MoS_2 nano-slits are made conductive *via* repetitive voltage cycling[34] with a 4 M LiCl solution (section 4 in the ESI†). The stable current *vs.* voltage (*I*–*V*) curve is shown in Fig. 2A. The device we report here has three conducting 2D nano-slits, each having the following dimensions: length (*L*) = 300 nm, width (*W*) = 100 nm, and height (*H*) = 8.4 nm; these dimensions are comparable to those of nano-slits (made *via* different fabrication routes) reported in the literature.[2,3] The theoretical conductance, *G*, is calculated using eqn (1), which turns out to be 1.46×10^{-7} S, where the experimental conductance for this device is 1.55×10^{-7} S. This shows that the device is stable and working as expected in the electrolyte solution (section 3 in the ESI†).

$$G = \frac{n\sigma WH}{L} \quad (1)$$

where *n* is the number of channels (*n* = 3 in this case), σ is the conductivity of the electrolyte,[35] which is 17.6 S m^{-1} for 4 M LiCl, *W* is the width, *H* is the height and *L* is the length of the 2D nano-slits.

The example of steady ionic current measured at different operating voltages is shown in Fig. 2B. The power spectral density (PSD) diagrams of the corresponding voltages are plotted and shown in Fig. 2C. As expected, the PSD diagram shows the typical pink/flicker noise and white noises[36] before getting cut off by the 100 kHz sampling frequency limit. As flicker noise (<100 Hz) is known to depend on device properties,[36,37] $1/f$ noise was further explored with our unique device architecture. In 2D channels, the flicker noise is known to deviate from empirical Hooge's law (eqn (2)). It follows the frequency relation (eqn (3)) in a low frequency regime (f < 100

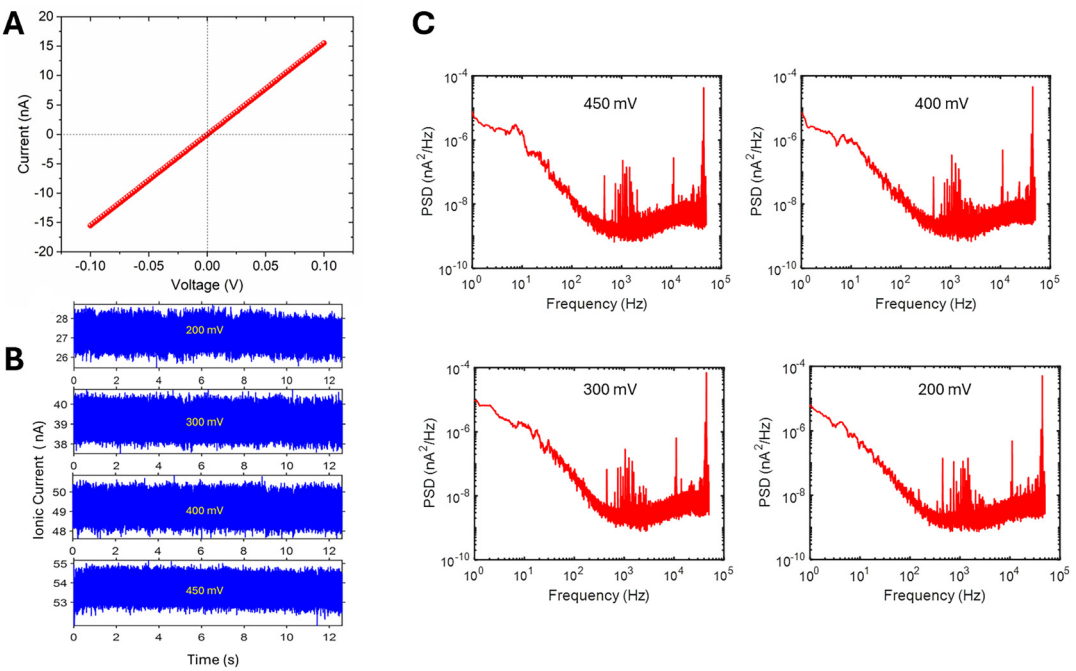

Fig. 2 (A) Current *vs.* voltage (*I*–*V*) curve of 2D nano-slits fabricated from MoS_2 nanocapillary in 4 M LiCl aqueous electrolyte. (B) Steady ionic current through 2D nano-slits at different operating voltages; the average current is shown in the *y*-axis and represented by dashed lines. (C) Power spectral density of the device at different operating voltages.

Hz), and the exponent (x) is known to depend on the channel properties.[37]

$$S_I(f) = \alpha \frac{I^2}{Nf} \quad (2)$$

Here, I is the ionic current, N is the number of ions inside the pore, and α is the numeric constant.

$$S_I \propto \frac{1}{f^x} \quad (3)$$

where $x = 1 + a$ and 'a' ranges from 0 to 0.5. According to Robin *et al.*,[37] for pristine graphite and pristine boron nitride, the exponent is reported as 1.3 and 1.2, respectively, whereas in our microtomy-fabricated MoS_2 2D nano-slits, the exponent value was found to be 1.5 by averaging over different voltage cases, as shown in Fig. S1.† The corresponding MATLAB codes used for data analysis can also be found in the ESI.†

The DNA (5 kbp linear dsDNA) translocation at a low voltage was dominated by spike events with this MoS_2-based 2D nano-slit device, consistent with the literature[2] (Fig. S6†). Spike events indicate the unsuccessful translocation of DNA, where the DNA tries to enter the nano-slit and withdraws due to an entropic barrier (Fig. 3C, section 5 in the ESI†). Furthermore, to overcome the entropic barrier, we have used a higher voltage of 400 mV for DNA translocation studies. Fig. 3A shows that we are able to detect the translocation of DNA through this nano-slit device in a non-destructive and label-free method. The representative figures of current blockades when a full DNA translocates through the slits are shown in Fig. 3B. This approach of using modulations in ionic current, inspired by the Coulter counter technique, is well known in the nanopore literature for characterization of the translocation of biomolecules.[38,39] For a first-order approximation, we have calculated the expected[40] current blockade when DNA translocates through the single nano-slit using eqn (4):

$$I_{\text{blockade}} = \frac{\sigma A V_{\text{bias}}}{L} \quad (4)$$

Here, σ is the conductivity of the electrolyte (17.6 S m^{-1} for 4 M LiCl solution), V_{bias} is the applied voltage bias (400 mV in this case), L is the length of the channel, which is 300 nm, and A is the effective cross-sectional area of the translocating molecule, where we approximated DNA as a cylinder with a maximum effective diameter of 2.3 nm.[41,42] The theoretical ionic current blockade calculated from eqn (4) is ~0.1 nA per single channel. We have found that the average ionic current blockade in our device with three 2D nano-slits is around 0.25 nA (Fig. 3E) for an applied voltage bias of 400 mV. These confirm DNA translocation through the 2D nano-slit with

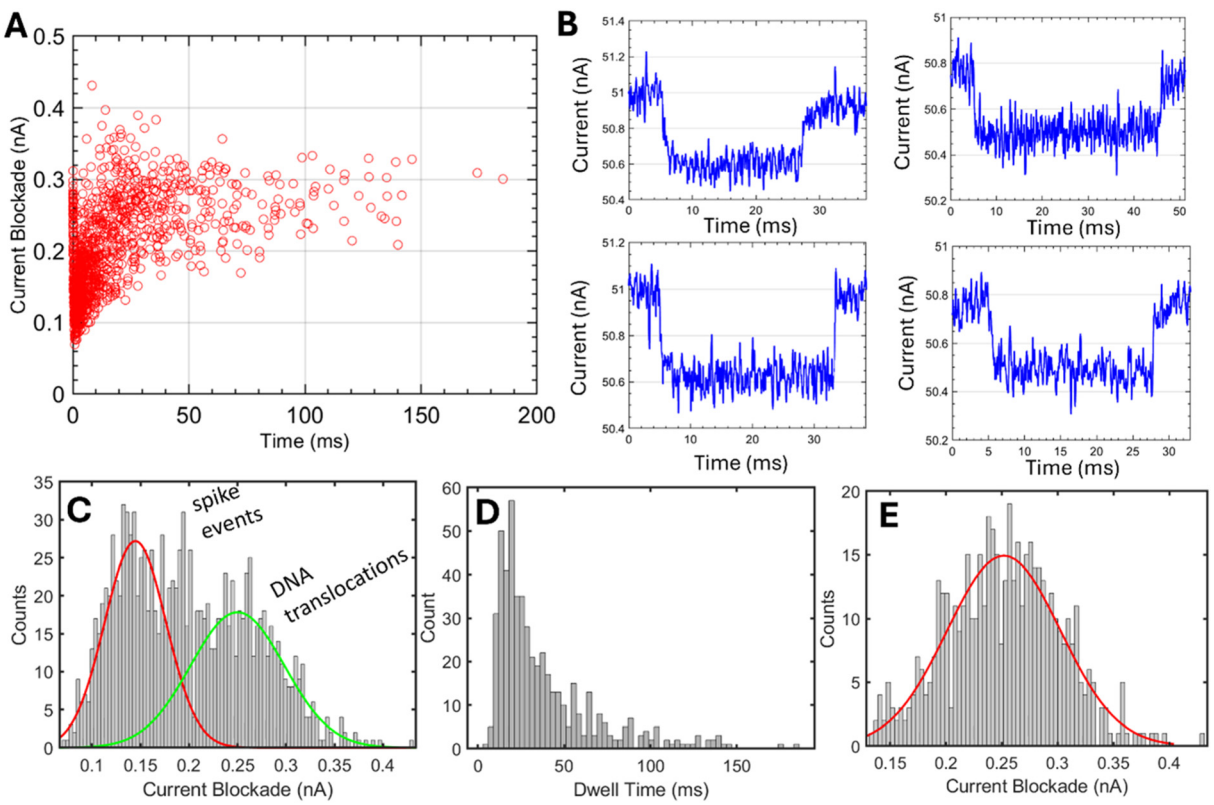

Fig. 3 (A) Current blockade *vs.* dwell time graph of DNA translocation through a 2D nano-slit device at 400 mV bias. (B) Representative current blockades of DNA translocating through a nano-slit. (C) Dwell time graph of DNA translocation and spike events. (D) Dwell time graph of DNA translocation events. (E) Gaussian-fitted current blockade graph of DNA translocation events.

various configurations such as loops, knots, folds, and so forth, as the nano-slit's height is more than three times DNA's diameter.

Under our measurement conditions (0.8 ng μL^{-1} of dsDNA in the reservoir in 4 M LiCl with an applied bias of 400 mV), the translocation event rate is lower than that of the solid-state nanopore.[26] However, this low event rate (less than one event per second) is similar to that reported in our previous study with graphene nano-slits.[2] Therefore, it is extremely unlikely to have simultaneous multi-DNA translocations through our device with MoS_2-based 2D nano-slits. These 2D nano-slits with MoS_2 walls show a median dwell time of ~27 ms (Fig. 3D), whereas a graphene nano-slit shows a median dwell time of ~8 ms, under different experimental conditions.[2] This could also be due to different entry/exit configurations of microtomy-fabricated MoS_2 2D nano-slits or DNA interactions with MoS_2 channel walls. Also, we have not observed any clogging of the nano-slit or permanent sticking of DNA inside the nano-slit device after the translocation measurements (Fig. S2†).

DNA topology investigations using MoS_2-based 2D nano-slits

The microtomy-fabricated 2D nano-slits with MoS_2 channel walls have a 2D constriction of ~8.4 nm, lower than the persistence length of DNA. As demonstrated in previous studies, translocation through these nano-slits compels DNA to shift from a 3D configuration to a 2D or 1D shape, inducing knots and folds or unwinding to a linear polymer. Understanding DNA and protein folding in such constrained environments has significant implications for biology, affecting processes from DNA replication and protein catalysis to the cellular mechanisms underlying folding. Gel electrophoresis is currently the major bulk technique used to study DNA knots, and

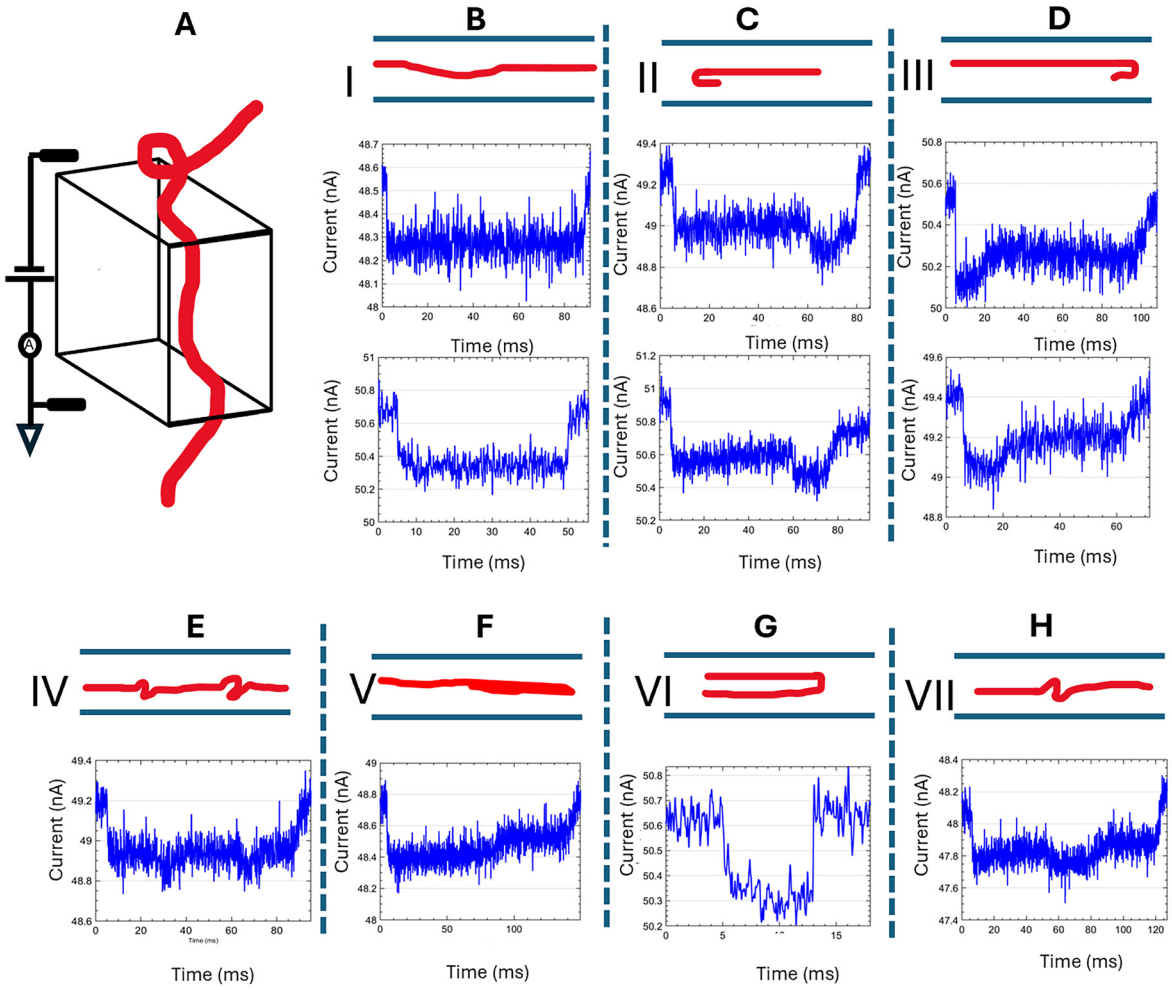

Fig. 4 Nano-slit microscopy for understanding the topology of DNA folding. (A) Schematic of DNA translocating through a 2D nano-slit. (B–H) Representative current blockades of DNA translocation in various configurations; unfolded DNA (I), semi-folded DNA on the left end (II), semi-folded DNA on the right end (III), two-times bent configuration in DNA (IV), partially folded DNA (V) and fully folded configuration (VI) and bent or partially folded DNA conformation (VII).

solid state nanopores were successfully used earlier to detect DNA knots.[43,44] Our studies using microtomy-fabricated MoS_2 2D nano-slits reveal direct observations of diverse DNA folding patterns, highlighting the potential of these devices for advanced biosensing applications.

In our earlier work,[2] we have demonstrated that the mechanically exfoliated graphene does not interact with double-stranded DNA owing to its atomically smooth and inert surface of basal planes with a negligible number of defects/surface charge. With the help of molecular dynamics simulation and related theoretical discussion, we have verified that the folding and knots remain undisturbed while translocating through the slit due to this negligible interaction.[2] Similarly, in this case, 2D nano-slits of MoS_2 did not show a significant interaction with DNA compared to the unconfined graphene.[45] As expected, the DNA has maintained the loop and folding while translocating through the slit (Fig. 4, Fig. S8 in the ESI†). As is known from previous works on ionic current-based sensing,[2,43,44] the shape of the ionic current blockade can be correlated to the 3D topology of DNA translocating through the pore/slit. Here, in MoS_2 nano-slits, the event rate is less than one event per second, and the chances of multiple DNA translocating together/tailgating are extremely low. Hence, building upon the simulation and theoretical studies in our previous work on DNA in nanoconfinement,[2] we assign the current blockade to the topology of DNA translocating through these 2D nano-slits. As shown in Fig. 4, we detected different possible conformations of DNA folding for the first time with MoS_2-based 2D nano-slits (section 6 in the ESI†). As the height of the slit is less than the persistence length of DNA ($H/L_p < 1$, where H is the height of the slit (8.4 nm) and L_p is the persistent length of DNA (~50 nm)), we are in the backfolded Odijk regime, and hence the type of folding, as shown in Fig. 4, is theoretically expected.[46] The probability distribution of different DNA foldings is provided in Fig. S9.† Moving forward, we aim to expand this investigation by exploring various device configurations and DNA lengths to further elucidate topological properties. We also hope to extend the application of this technique for studying G-quadruplexes, R-loops and other disease-relevant DNA folding and structural variations.

Conclusions

We demonstrated the biosensing capabilities of 2D nano-slits with MoS_2 channel walls fabricated using a scalable ultramicrotomy technique and showed their applications in DNA sensing. We also report the deviation of $1/f$ noise from empirical Hooge's law with an exponent value of 1.5. To explore the biosensing capabilities of our devices, we conducted electrophysiological testing using microtomy-fabricated MoS_2 2D nano-slits. These measurements enabled real-time monitoring of ionic current fluctuations during DNA translocation, allowing us to directly observe distinct folding configurations. The high sensitivity and spatial resolution of these nano-slits underscore their potential for advanced single-molecule analysis and next-generation biosensing applications. This work, through sustainable and scalable fabrication of nano-slit devices with precise dimensions, paves the way to advance nano-slit technologies for applications in proteomics to an integral part of point-of-care devices. Currently, we are exploring the potential of these robust microtomy-fabricated, chemically tunable MoS_2 devices for selective biomolecule sensing and size-based filtering of biomolecules.

Data availability

The data supporting this article have been included as part of the ESI.† The GitHub links for all the codes used are also added in the ESI.†

Conflicts of interest

There are no conflicts to declare.

Acknowledgements

A. K. acknowledges the Royal Society grant ICA\R1\231014, and the Presidential Fellowship from the University of Manchester. B. R. acknowledges funding from the European Union's H2020 Framework Programme/European Research Council Starting Grant (852674 – AngstroCAP), the Royal Society University Research Fellowship (URF\R1\180127, URF\R\231008), Philip Leverhulme Prize PLP-2021-262, and EPSRC New Horizons grant EP/X019225/1. B. R. and A. K. acknowledge EPSRC strategic equipment grant EP/W006502/1. M. S. P. acknowledges the Commonwealth Split-Site PhD Scholarship and the UoM-IISc joint degree studentship award. This work was partly supported by the Scientific and Useful Profound Research Advancement (SUPRA) Program of the Science Engineering Research Board (SERB) under grant SPR/2021/000275. AK acknowleges the UK-India Education Research Innovation (UKIERI) award supported by the British Council (IND/CONT/G/23-24/37).

References

1 J. Reitemeier, J. Metro and K. X. Fu, Nanopore sensing and beyond: Electrochemical systems for optically-coupled single-entity studies, stimulus-responsive gating applications, and point-of-care sensors, *Sens. Actuators Rep.*, 2024, **8**, 100225.
2 W. Yang, *et al.*, Translocation of DNA through Ultrathin Nanoslits, *Adv. Mater.*, 2021, **33**, 2007682.
3 Y. Cui, *et al.*, Electrical Transport and Dynamics of Confined DNA through Highly Conductive 2D Graphene Nanochannels, *Nano Lett.*, 2024, **24**, 4485–4492.

4 M. E. Gracheva, *et al.*, Simulation of the electric response of DNA translocation through a semiconductor nanopore–capacitor, *Nanotechnology*, 2006, **17**, 622–633.
5 U. F. Keyser, *et al.*, Direct force measurements on DNA in a solid-state nanopore, *Nat. Phys.*, 2006, **2**, 473–477.
6 A. Dorey and S. Howorka, Nanopore DNA sequencing technologies and their applications towards single-molecule proteomics, *Nat. Chem.*, 2024, **16**, 314–334.
7 H. Brinkerhoff, A. S. W. Kang, J. Liu, A. Aksimentiev and C. Dekker, Multiple rereads of single proteins at single–amino acid resolution using nanopores, *Science*, 2021, **374**, 1509–1513.
8 K. Motone, *et al.*, Multi-pass, single-molecule nanopore reading of long protein strands, *Nature*, 2024, **633**, 662–669.
9 F. Wang, *et al.*, MoS2 nanopore identifies single amino acids with sub-1 Dalton resolution, *Nat. Commun.*, 2023, **14**, 2895.
10 M. Iarossi, N. C. Verma, I. Bhattacharya and A. Meller, The Emergence of Nanofluidics for Single-Biomolecule Manipulation and Sensing, *Anal. Chem.*, 2025, **97**, 8641–8653.
11 M. Sajeer P, Simran, P. Nukala and M. M. Varma, TEM based applications in solid state nanopores: From fabrication to liquid *in situ* bio-imaging, *Micron*, 2022, **162**, 103347.
12 A. J. Storm, J. H. Chen, X. S. Ling, H. W. Zandbergen and C. Dekker, Fabrication of solid-state nanopores with single-nanometre precision, *Nat. Mater.*, 2003, **2**, 537–540.
13 P. M. Sajeer, A. Keerthi and M. Varma, Solid-state nanopore conductance modulation using integrated microheaters, *Nanotechnology*, 2025, **36**, 265301.
14 K. Fu, S.-R. Kwon, D. Han and P. W. Bohn, Single Entity Electrochemistry in Nanopore Electrode Arrays: Ion Transport Meets Electron Transfer in Confined Geometries, *Acc. Chem. Res.*, 2020, **53**, 719–728.
15 A. Bhardwaj, *et al.*, Fabrication of angstrom-scale two-dimensional channels for mass transport, *Nat. Protoc.*, 2024, **19**, 240–280.
16 T. Emmerich, *et al.*, Nanofluidics, *Nat. Rev. Methods Primers*, 2024, **4**, 69.
17 Editorial, Nanofluidics is on the rise, *Nat. Mater.*, 2020, **19**, 253.
18 A. Bhardwaj, *et al.*, Ultramicrotomy–Assisted Fabrication of Nanochannels for Efficient Ion Transport and Energy Generation, *Adv. Funct. Mater.*, 2024, 2401988, DOI: 10.1002/adfm.202401988.
19 B. Radisavljevic, A. Radenovic, J. Brivio, V. Giacometti and A. Kis, Single-layer MoS2 transistors, *Nat. Nanotechnol.*, 2011, **6**, 147–150.
20 N. A. Kumar, M. A. Dar, R. Gul and J.-B. Baek, Graphene and molybdenum disulfide hybrids: synthesis and applications, *Mater. Today*, 2015, **18**, 286–298.
21 S. Bharti, S. K. Tripathi and K. Singh, Recent progress in MoS2 nanostructures for biomedical applications: Experimental and computational approach, *Anal. Biochem.*, 2024, **685**, 115404.
22 M. C. Rodríguez González, *et al.*, Clicking beyond suspensions: understanding thiol–ene chemistry on solid-supported MoS_2, *Nanoscale*, 2024, **16**, 3749–3754.
23 A. B. Farimani, K. Min and N. R. Aluru, DNA Base Detection Using a Single-Layer MoS_2, *ACS Nano*, 2014, **8**, 7914–7922.
24 Z. Cao, P. Yadav and A. Barati Farimani, Which 2D Material is Better for DNA Detection: Graphene, MoS_2, or MXene?, *Nano Lett.*, 2022, **22**, 7874–7881.
25 H. Chen, *et al.*, Protein Translocation through a MoS_2 Nanopore:A Molecular Dynamics Study, *J. Phys. Chem. C*, 2018, **122**, 2070–2080.
26 J. Feng, *et al.*, Identification of single nucleotides in MoS2 nanopores, *Nat. Nanotechnol.*, 2015, **10**, 1070–1076.
27 K. Liu, J. Feng, A. Kis and A. Radenovic, Atomically Thin Molybdenum Disulfide Nanopores with High Sensitivity for DNA Translocation, *ACS Nano*, 2014, **8**, 2504–2511.
28 D. Sarkar, *et al.*, MoS_2 Field-Effect Transistor for Next-Generation Label-Free Biosensors, *ACS Nano*, 2014, **8**, 3992–4003.
29 M. Graf, M. Lihter, D. Altus, S. Marion and A. Radenovic, Transverse Detection of DNA Using a MoS_2 Nanopore, *Nano Lett.*, 2019, **19**, 9075–9083.
30 P. Cadinu, *et al.*, Double Barrel Nanopores as a New Tool for Controlling Single-Molecule Transport, *Nano Lett.*, 2018, **18**, 2738–2745.
31 X. Liu, Y. Zhang, R. Nagel, W. Reisner and W. B. Dunbar, Controlling DNA Tug–of–War in a Dual Nanopore Device, *Small*, 2019, **15**, 1901704.
32 S. W. Kowalczyk, D. B. Wells, A. Aksimentiev and C. Dekker, Slowing down DNA Translocation through a Nanopore in Lithium Chloride, *Nano Lett.*, 2012, **12**, 1038–1044.
33 C. Plesa and C. Dekker, Data analysis methods for solid-state nanopores, *Nanotechnology*, 2015, **26**, 084003.
34 S. Goutham, R. K. Gogoi, H. Jyothilal, G.-H. Nam, A. Ismail, S. V. Pandey, A. Keerthi and B. Radha, Electric field mediated unclogging of Angstrom-scale Channels, *Small Methods*, 2025, **9**, 2400961.
35 J. Saharia, *et al.*, Modulation of electrophoresis, electroosmosis and diffusion for electrical transport of proteins through a solid-state nanopore, *RSC Adv.*, 2021, **11**, 24398–24409.
36 A. Fragasso, S. Schmid and C. Dekker, Comparing Current Noise in Biological and Solid-State Nanopores, *ACS Nano*, 2020, **14**, 1338–1349.
37 P. Robin, *et al.*, Disentangling 1/*f* noise from confined ion dynamics, *Faraday Discuss.*, 2023, **246**, 556–575.
38 M. Muthukumar, C. Plesa and C. Dekker, Single-molecule sensing with nanopores, *Phys. Today*, 2015, **68**, 40–46.
39 A. Dominic, M. Sajeer Parambath, S. Nasa and M. Varma, Practical guide for in-house solid-state nanopore fabrication and characterization, *J. Vac. Sci. Technol., B: Nanotechnol. Microelectron.:Mater., Process., Meas., Phenom.*, 2023, **41**, 043204.
40 P. Chen, *et al.*, Probing Single DNA Molecule Transport Using Fabricated Nanopores, *Nano Lett.*, 2004, **4**, 2293–2298.

41 S. Garaj, S. Liu, J. A. Golovchenko and D. Branton, Molecule-hugging graphene nanopores, *Proc. Natl. Acad. Sci. U. S. A.*, 2013, **110**, 12192–12196.
42 R. K. Sharma, I. Agrawal, L. Dai, P. Doyle and S. Garaj, DNA Knot Malleability in Single-Digit Nanopores, *Nano Lett.*, 2021, **21**, 3772–3779.
43 R. Kumar Sharma, I. Agrawal, L. Dai, P. S. Doyle and S. Garaj, Complex DNA knots detected with a nanopore sensor, *Nat. Commun.*, 2019, **10**, 4473.
44 C. Plesa, *et al.*, Direct observation of DNA knots using a solid-state nanopore, *Nat. Nanotechnol.*, 2016, **11**, 1093–1097.
45 S. Banerjee, *et al.*, Slowing DNA Transport Using Graphene–DNA Interactions, *Adv. Funct. Mater.*, 2015, **25**, 936–946.
46 K. Frykholm, V. Müller, S. Kk, K. D. Dorfman and F. Westerlund, DNA in nanochannels: theory and applications, *Q. Rev. Biophys.*, 2022, **55**, e12.